

# GSA Data Repository 2015246

## $^{40}\text{Ar}/^{39}\text{Ar}$ ANALYTICAL METHODS

Visible alteration was first removed from selected dredge samples using a rock saw. The freshest material was then crushed and incrementally ground and sieved into size fractions between 63 and 30/32  $\mu\text{m}$ . Feldspar separates were then prepared using a combination of heavy liquid and paramagnetic methods, cleaned with 2% HF (15 min), and 6N HCl (60 min), 1N HNO<sub>3</sub> (60 min), untra-pure H<sub>2</sub>O (60 min), all in an ultrasonic bath @ 50°C.

The 300-200 micron groundmass sample was prepared by incremental crushing and sieving, magnetic separation, and cleaning with 6N HCl (60 min), 1N HNO<sub>3</sub> (60 min), untra-pure H<sub>2</sub>O (60 min), all in an ultrasonic bath @ 50°C , as described in Koppers et al (2000).

Mineral separates and the groundmass sample were irradiated in the cadmium-shielded facility in the cadmium-lined position in the Petten reactor. Samples were incrementally heated using a continuous 15W CO<sub>2</sub> laser connected to a MAP-215/50 mass spectrometer at the VU University Amsterdam.

Data acquisition and reduction, corrections for mass discrimination and age calculation have been described in detail previously (Koppers et al., 2000; Koppers, 2002; O'Connor et al., 2004, Kuiper et al., 2008). Incremental heating plateau ages and isochron ages were calculated as weighted means with  $1/\sigma^2$  as weighting factor (Taylor, 2003) and as YORK2 least squares fits with correlated errors (York, 1969) using the ArArCalc v. 2.50a software from Koppers (2002)that is available from the <http://earthref.org/tools/ararcalc.htm> Web site.

Sample information in Table DR1,  $^{40}\text{Ar}/^{39}\text{Ar}$  results in Table DR2, age and K/Ca spectra in Fig. DR3, analytical methods in dataset DR4, and ArArCalc Excel data files in DR5. The details of the ArArCalc tables and plots are explained in full in Koppers et al (2012). Typical J-value error is 0.3% at  $1\sigma$ . Ages are calculated using a Drachenfels sanidine (internal laboratory standard DRA-1;  $25.26 \pm 0.6$  Ma (modified after Wijbrans et al., 1995), intercalibrated against TCR-1 sanidine at 28.34 Ma (Renne et al., 1998), decay constants of Steiger & Jaeger (1977) and the following correction factors for the Petten reactor:  $^{40}\text{Ar}/^{39}\text{Ar}$  (K) =  $0.00183 \pm 0.00107$ ,  $^{36}\text{Ar}/^{37}\text{Ar}$  35 (Ca) =  $0.000265 \pm 0.000008$ ,  $^{39}\text{Ar}/^{37}\text{Ar}$  (Ca) =  $0.000699 \pm 0.000033$ .

## Data Quality

The  $^{40}\text{Ar}/^{39}\text{Ar}$  ages reported here meet the following acceptability criteria and thresholds (after Fleck et al., 1977, Lanphere and Dalrymple, 1978; Dalrymple et al., 1980, Pringle, 1993) and are therefore accepted as reliably dating the solidification of the volcanic rocks immediately after eruption.

- A well-defined high-temperature age spectrum plateau is created by three or more concordant (within  $2\sigma$ ), with contiguous steps representing at least 50% of the  $^{39}\text{Ar}$  released. Plateaus reported here contain at least 90% of the total released  $^{39}\text{Ar}$
- The plateau and isochron ages should be concordant at the 95% confidence level

- In all cases the total fusion age agrees with the both the calculated plateau and inverse isochron ages
- The mean square of weighted deviations (York, 1969; Roddick, 1978) for both the plateau ages (MSWD =SUMS/N-1) and isochron ages (MSWD = SUMS/ N-2) should be sufficiently small if compared to Student's t-test and F-statistic critical values for significance, respectively.

## REFERENCES

- Cande, S.C., LaBrecque, J.L., Larson, R.L. Pitmann III, W.C., Golovchenko, X. and Haxby, W.F., 1989, Magnetic Lineations of the World's Ocean Basins (map). Scale: approximately 1:27,400,000 at the equator: *American Association of Petroleum Geologists*, Tulsa, Okla.
- Dalrymple, G.B., Lanphere, M.A. and Clague, D.A., 1980, Conventional and  $^{40}\text{Ar}/^{39}\text{Ar}$  ages of volcanic rocks from Ojin (Site 430), Nintoku (Site 432), and Suiko (Site 433) Seamounts and the chronology of volcanic propagation along the Hawaiian-Emperor chain: *Initial Rep. Deep Sea Drill. Proj.* v. 55, p. 659–676.
- Fleck, R.J., Sutter, J.F., Elliot, D.H., 1977, Interpretation of discordant  $^{40}\text{Ar}/^{39}\text{Ar}$  age spectra of Mesozoic tholeiites from Antarctica: *Geochim. Cosmochim. Acta*, v. 41, p. 15-32.
- Koppers, A.A.P., Staudigel, H. and Wijbrans, J.R., 2000, Dating crystalline groundmass separates of altered Cretaceous seamount basalts by the  $^{40}\text{Ar}/^{39}\text{Ar}$  incremental heating technique: *Chemical Geology*, v. 166, p. 139-158, doi:10.1016/S0009-2541(99)00188-6.
- Koppers, A.A.P., 2002, ArArCALC – software for  $^{40}\text{Ar}/^{39}\text{Ar}$  age calculations: *Computers Geosciences*, v. 5, p. 605–619, doi:10.1016/S0098-3004(01)00095-4.
- Koppers, A.A.P., Yamazaki, T., Geldmacher, J., Gee, J.S., Pressling, N., Hoshi, H. et al., 2012, Limited latitudinal mantle plume motion for the Louisville hotspot: *Nature Geoscience*, v. 5, p. 911-917, doi: 10.1038/ngeo1638.
- Kuiper, K.F., Deino, A., Hilgen, F.J., Krijgsma, W., Renne, P.R. and Wijbrans, J.R., 2008, Synchronizing Rock Clocks of Earth History: *Science*, v. 320, p. 500-504, doi: 10.1126/science.1154339.
- Lanphere, M.A., Dalrymple, G.B., 1978, The use of  $^{40}\text{Ar}/^{39}\text{Ar}$  data in evaluation of disturbed K–Ar systems: Short Papers 4th Int. Conf. Geochronol. Cosmochronol. Isot. Geol., v. 78–701, pp. 241–243.
- O'Connor, J.M., Stoffers, P. and Wijbrans, J.R., 2004, The Foundation Chain: Inferring hotspot-plate interaction from a weak seamount trail, in Hekinian, R., Stoffers, P. and Cheminée J.-L. (eds), *Oceanic Hotspots*, Springer, Berlin, Heidelberg, New York, p. 349-372,
- Pringle, M.S., 1993, The Mesozoic Pacific: geology, tectonics, and volcanism: *Geophys. Monogr.*, v. 77, p. 187–215.
- Renne, P.R., Swisher, C.C., Deino, A.L., Karner, D.B., Owens, T.L. and DePaolo, D.J., 1998, Intercalibration of standards, absolute ages and uncertainties in  $^{40}\text{Ar}/^{39}\text{Ar}$  dating: *Chemical Geology*, v. 145, p. 117–152.
- Roddick, J.C., 1978, The application of isochron diagrams in  $^{40}\text{Ar}/^{39}\text{Ar}$  dating: A discussion: *Earth Planet. Sci. Lett.*, v. 41, p. 233–244.
- Sandwell, D.T. and Smith W.H.F., 2009, Global marine gravity from retracked Geosat and ERS-1 altimetry: Ridge segmentation versus spreading rate: *J. Geophys. Res.*, v. 114, B01411, doi:10.1029/2008JB006008.
- Steiger, R.H. and Jaeger, E., 1977, Subcommission on Geochronology: convention on the use of decay constants in Geo and Cosmochronology: *Earth Planet. Sci. Lett.*, v.36, p. 359-362.
- Taylor, J.R., 2003, An Introduction to Error Analysis: 327 pp., Univ. Sci. Books, Mill Valley, Calif.
- Wijbrans, J.R., Pringle, M.S. Koppers, A.A.P. and Scheevers, R., 1995, Argon geochronology of small samples using the Vulkaan argon laserprobe: *Proc. Kon. Ned. Akad. Wet.*, 98, p. 185–218.
- York, D., 1969, Least squares fitting of a straight line with correlated errors: *Earth Planet. Sci. Lett.*: v. 5, p. 320–324.

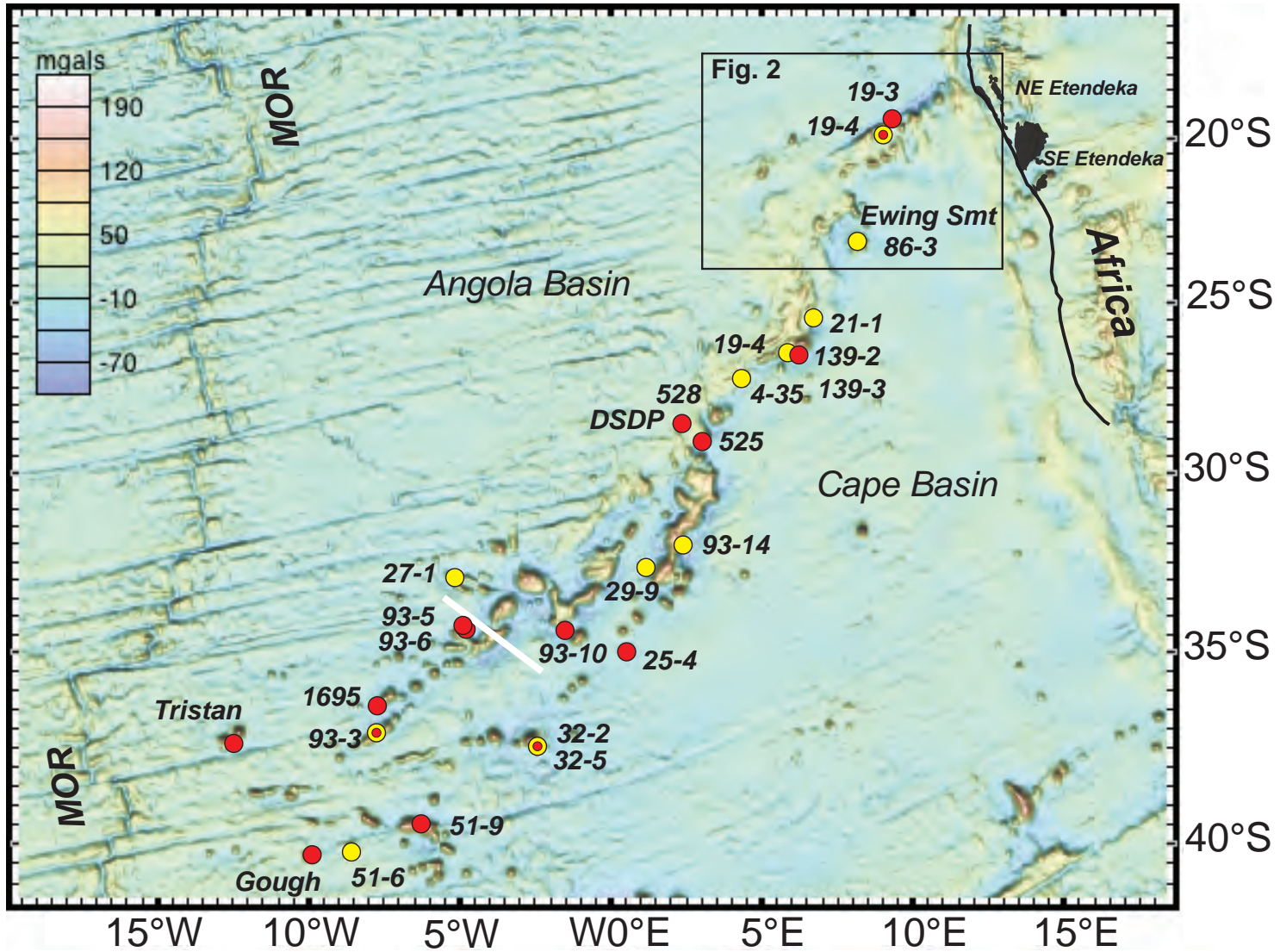


Figure DR1a. Free air gravity field map for the southeast Atlantic (Sandwell and Smith, 2009) showing the basement structure of the Walvis Ridge. The yellow circles are for the locations of samples dated for this study (Tables DR1 and DR2). The locations of samples with published ages used in this study are shown as red circles (O'Connor & le Roex, 1992; Maund et al 1988; Rohde et al., 2012; Hicks et al., 2012). White line is for a seismic refraction profile discussed in the text. MOR = Mid-Ocean Ridge. Northern and Southern Etendeka flood basalts are shown as dark areas (after Ewart et al., 2004). Maps prepared using GeoMapApp (<http://www.geomapapp.org>).

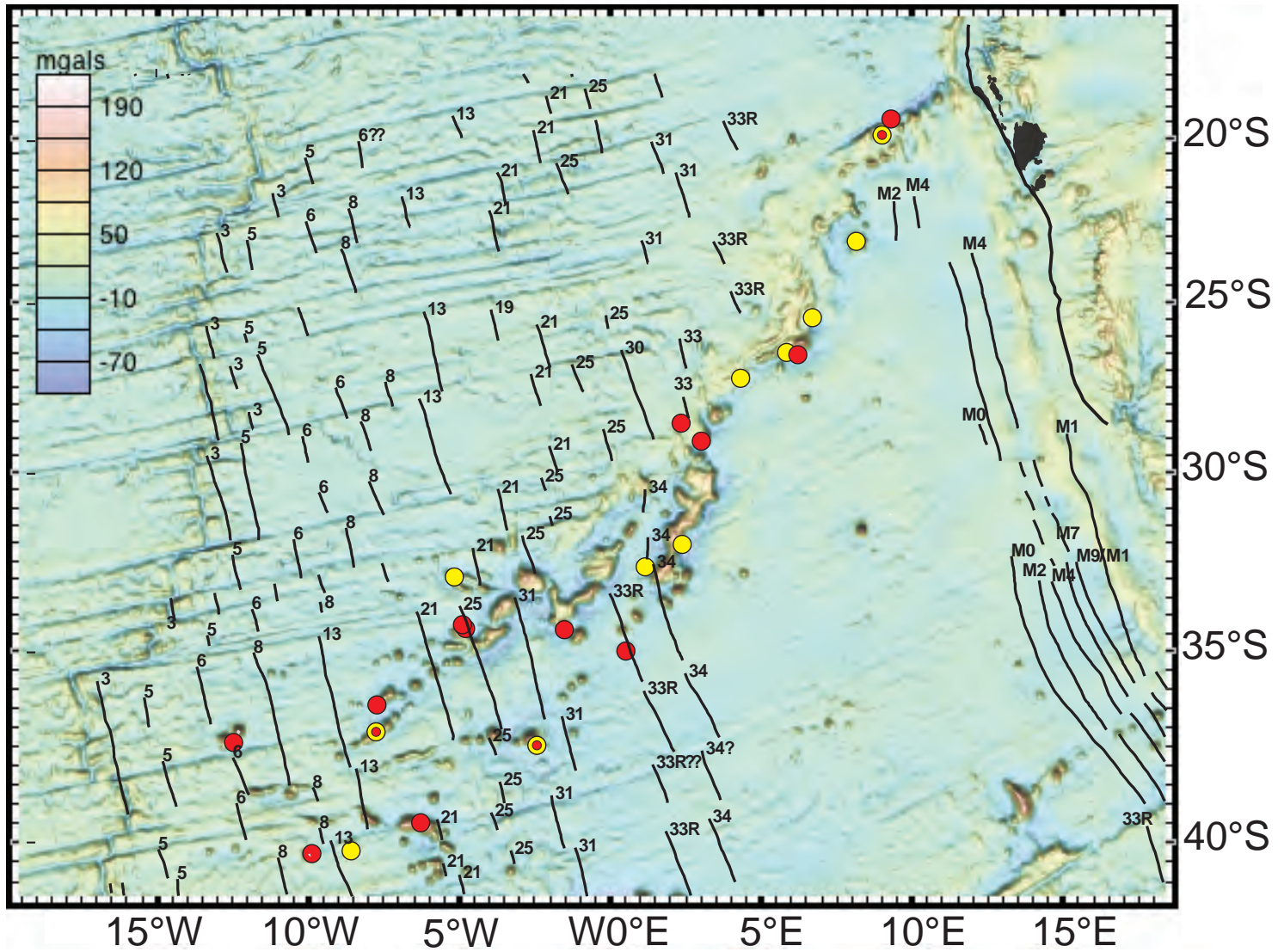


Figure DR1b. Comparison between Fig. DR1a gravity map and seafloor magnetic isochrons (Cande et al., 1989).

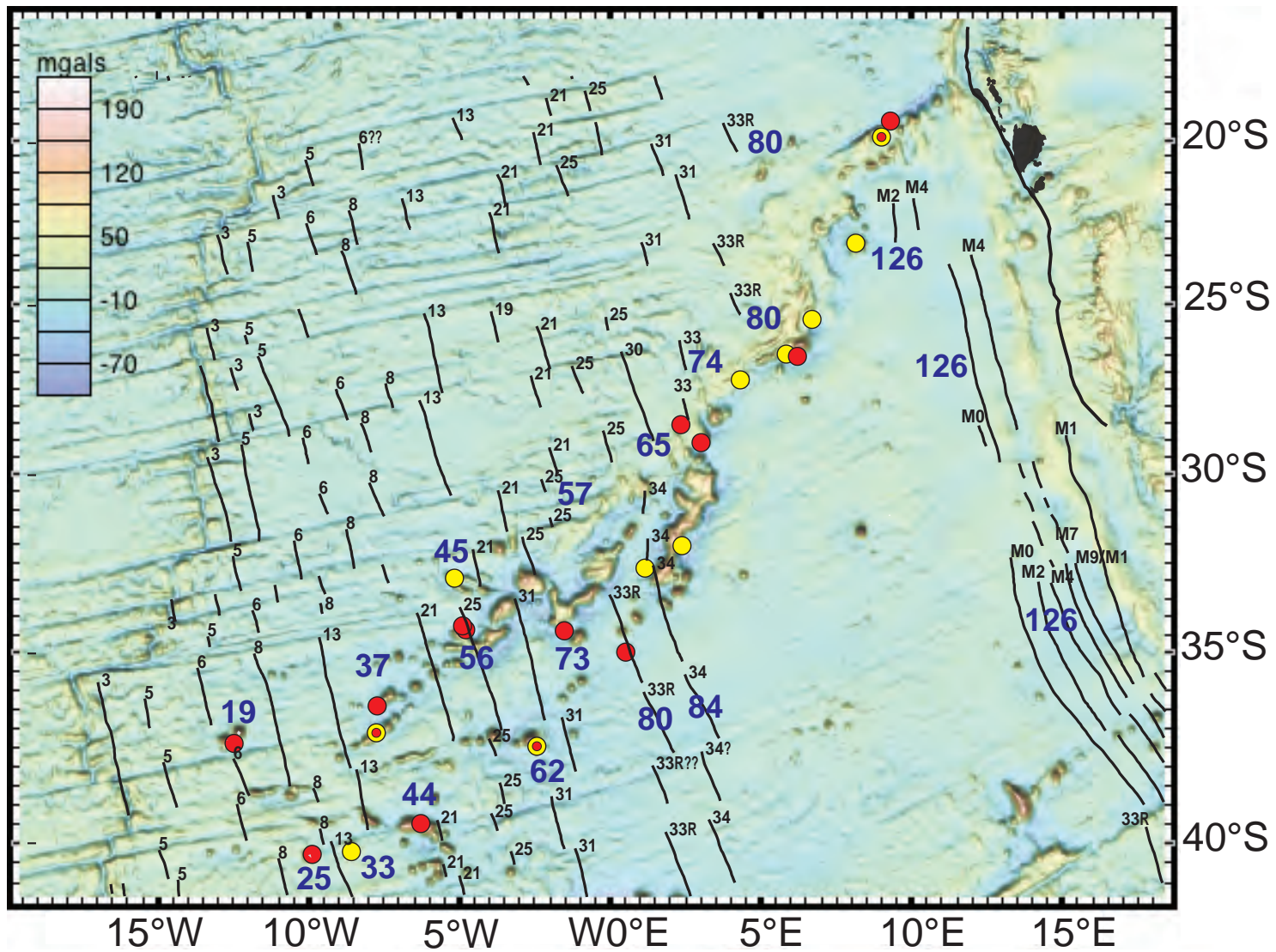


Figure DR1c. Estimated plate age (Ma) at eruption time shown as large blue numbers. Note that the oceanic crust is roughly 20 Ma older on the northern side of the Walvis Ridge than on the southern side. This plate boundary provided lines of weakness for plume material to reach the surface such as existing fracture in close proximity to a slowly migrating spreading ridge (see text for discussion).

**Table DR1. Summary of sample information and  $^{40}\text{Ar}/^{39}\text{Ar}$  ages**

Sample	Latitude ( $^{\circ}$ )	Longitude ( $^{\circ}$ )	Depth (mbsl)	Age (Ma)	$2\sigma$	Description	Location
WALDA-002-CH19-DR4-03	-19.85	9.02	2738	112.1	$\pm 0.3$	Basaltic trachyandesite <sup>1</sup>	NE Walvis
-CH19-DR4-1	-19.86	9.02	2738	112.2	$\pm 0.7$	Basaltic trachyandesite <sup>1</sup>	NE Walvis
SO84 86DS-3 ( <i>Ewing Smt</i> )	-23.11	8.16	2193-2918	72.7	$\pm 1.2$		Central Walvis ( <i>Ewing Smt.</i> )
AII-93-21-1	-25.44	6.70	3160-2625	57.0	$\pm 0.7$	Trachyte <sup>1</sup>	Central Walvis
CIR139D-2	-26.50	5.88	3480	78.4	$\pm 0.5$	tholeiitic basalt <sup>3</sup>	Central Walvis
CIR 139D-3	-26.50	5.88	3480	78.6	$\pm 0.3$	tholeiitic basalt <sup>3</sup>	Central Walvis
Walvis III DR04-35	-27.24	4.38	3295-2660	66.4	$\pm 0.6$	trachybasalt <sup>3</sup>	Central Walvis
AII-93-14-19	-31.99	2.39	2304-1587	59.3	$\pm 0.2$	Mugearite <sup>2</sup>	Bifurcated Ridges
AII-93-14-1	-31.99	2.39	2304-1587	59.0	$\pm 0.2$	Mugearite <sup>2</sup>	Bifurcated Ridges
Vema 29-9-1	-32.63	1.12	3510	61.5	$\pm 0.4$	Alkali basalt <sup>3</sup>	Bifurcated Ridges
PS69-435-1-DR27-1	-32.89	-5.15	2404-2291	36.5	$\pm 0.7$	Alkali basalt <sup>2</sup>	Bifurcated Ridges
PS69-440_1-DR32-2	-37.48	-2.43	1895-1390	37.4	$\pm 0.2$	Trachybasalt <sup>1</sup>	Smt. Province
PS69-440-1-DR32-5b	-37.48	-2.43	1895-1390	36.9	$\pm 0.4$	Trachybasalt <sup>1</sup>	Smt. Province
AII-93-3-1B	-37.10	-7.78	2600-2000	27.4	$\pm 0.7$	Alkali basalt <sup>2</sup>	Smt. Province
AG51-6-1	-40.17	-8.55		7.1	$\pm 0.1$	Tephrite <sup>2</sup>	Smt. Province (McNish Smt.)

<sup>1</sup>Rohde et al., 2012<sup>2</sup>Rohde et al., 2013<sup>3</sup>J. Rohde, personal communication, 2014

Samples analyzed in this study were collected as follows:

U.S.A. R/V Atlantis II expedition (samples AII-93) in 1975

U.S.A. R/V Vema expedition Vema 29 in 1972

U.S.A. R/V Argo expedition 'Circe' (dredge sample CIR139) in 1968

French R/V Jean Charcot cruise WALDA-002 (samples CH19) in 1971 (Hekinian, 1971)

French R/V Jean Charcot cruise WALVIS CH86 (Walvis III) (sample DR04) in 1979

German R/V Sonne SO84 expedition in 1993 (Devey et al., 1993)

German R/V Polarstern ANTXXIII-5 (PS69) expedition in 2006 (Jokat, 2008)

South African R/V Agulhas expedition AG51 in 1987

Devey et al., 1993, Cruise report SO-84: The St Helena hotspot: *Reports Geol.-Paläont. Inst. Univ. Kiel*, v. 64, 103 pp.Hekinian, R., 1971, Volcanics from the Walvis Ridge: *Nature*, v. 239, p. 91-93.Jokat, W., 2008, The south Atlantic expedition ANT-XXIII/5 of the research vessel "Polarstern" in 2006: *Reports on Polar and Marine Res.*, v. 574, 110 pp.

German R/V Sonne SO84 expedition in 1993 (Devey et al., 1993)

German R/V Polarstern ANTXXIII-5 (PS69) expedition in 2006 (Jokat, 2008)

South African R/V Agulhas expedition AG51 in 1987

**Table DR2.**  $^{40}\text{Ar}/^{39}\text{Ar}$  analyses of dredge sampled lavas from the Walvis Ridge

Sample	Lab ID	Plateau age					Total Fusion		Inverse Isochron Analysis		
		Age (Ma)	% $^{39}\text{Ar}$	K/Ca	MSWD <sup>a</sup>	n <sup>b</sup>	Age (Ma)	Age (Ma)	$^{40}\text{Ar}/^{36}\text{Ar}$ Intercept	MSWD <sup>a</sup>	Type
WALDA-002-CH19-DR4-3	12M0287	112.1 ± 0.4	100	0.07	0.3	14	112.1 ± 0.4	112.1 ± 0.3	294 ± 3	0.3	B. trachyanesite
WALDA-002-CH19-DR4-1	12M0293	112.2 ± 0.6	97	0.03	0.2	13	112.3 ± 0.6	112.2 ± 0.7	295 ± 35	0.2	B. trachyanesite
SO84 86DS-3 <sup>c</sup>	12M0397	72.8 ± 1.6	91	0.01	0.03	11	76.4 ± 3.4	72.7 ± 1.2	296 ± 4	0.01	
AII-93-21-1	12M0294	57.6 ± 0.5	96	0.03	0.4	11	58.0 ± 0.5	57.0 ± 0.7	368 ± 74	0.3	Trachyte
CIR139D-2	12M0290	78.4 ± 0.9	100	0.02	0.4	13	78.2 ± 0.9	78.4 ± 0.5	293 ± 13	0.4	Tholeiitic basalt
CIR 139D-3	12M0292	78.6 ± 0.5	100	0.03	0.3	12	78.6 ± 0.6	78.6 ± 0.3	294 ± 5	0.3	Tholeiitic basalt
Walvis III DR04-35	12M0289	66.8 ± 0.9	100	0.02	0.4	14	66.9 ± 1.1	66.4 ± 0.6	312 ± 9	0.1	trachybasalt
AII-93-14-19	12M0300	59.3 ± 0.3	95	0.05	0.2	12	59.3 ± 0.3	59.3 ± 0.2	291 ± 5	0.1	Mugearite
AII-93-14-1	12M0309	59.0 ± 0.2	100	0.09	0.4	13	59.1 ± 0.2	59.0 ± 0.2	302 ± 11	0.4	Mugearite
Vema 29-9-1	12M0297	61.5 ± 0.6	100	0.02	0.2	13	61.6 ± 0.7	61.5 ± 0.4	296 ± 4	0.2	Alkali basalt
PS69-4350-1-DR27-1	12M0303	36.7 ± 1.2	100	0.01	0.1	13	36.6 ± 1.2	36.5 ± 0.7	299 ± 9	0.1	Alkali basalt
PS69-440_1-DR32-2	12M0298	37.4 ± 0.3	100	0.05	0.1	13	37.4 ± 0.3	37.4 ± 0.2	297 ± 4	0.1	Trachybasalt
PS69-440-1-DR32-5b	12M0299	37.1 ± 0.3	100	0.05	0.1	13	37.1 ± 0.3	36.9 ± 0.4	300 ± 12	0.1	Trachybasalt
AII-93-3-1B	12M0302	27.4 ± 1.4	100	0.01	0.2	13	27.6 ± 1.6	27.4 ± 0.7	295 ± 3	0.2	Alkali basalt
AG51-6-1 <sup>d</sup>	12M0311	7.1 ± 0.1	93	0.39	0.03	10	7.1 ± 0.1	7.1 ± 0.1	296 ± 28	0.02	Tephrite

All samples except are HF leached (2% for 15 mins) 63-30/32  $\mu\text{m}$  plagioclase separates except for c and d

Ages are calculated using DRA monitor age of  $25.26 \pm 0.6$  Ma (Wijbrans et al., 1995), intercalibrated against TCR-1 sanidine at 28.34 Ma (Renne et al., 1998), and the decay constant of Steiger & Jaeger (1977)

Typical J-value error is 0.3% at  $1\sigma$ .

$^{40}\text{Ar}/^{39}\text{Ar}$  ages were measured using the argon laser probe at VU University Amsterdam

Measured ages have been calculated using the Freeware software ArArCalc (Koppers et al., 2002)

ArArCALC data are available in Data Repository

$\lambda = 5.543 \times 10^{-10}/\text{yr}$

Correction factors:

$^{40}\text{Ar}/^{39}\text{Ar}$  (K) =  $0.00183 \pm 0.00107$

$^{36}\text{Ar}/^{37}\text{Ar}$  (Ca) =  $0.000265 \pm 0.000008$

$^{39}\text{Ar}/^{37}\text{Ar}$  (Ca) =  $0.000699 \pm 0.000033$

<sup>a</sup>MSWD values for the plateaus and inverse isochrons are calculated using N-1 and N-2 degrees of freedom, respectively.

<sup>b</sup>n is for the number of included heating steps

<sup>c</sup>Groundmass 300-200  $\mu\text{m}$  separate

<sup>d</sup> = Alkali feldspar

Koppers, A. A. P., 2002, ArArCALC – software for  $^{40}\text{Ar}/^{39}\text{Ar}$  age calculations: *Computers Geosciences*, v. 5, p. 605–619.

Renne, P.R., Swisher, C.C., Deino, A.L., Karner, D.B., Owens, T.L. and DePaolo, D.J., 1998, Intercalibration of standards, absolute ages and uncertainties in  $^{40}\text{Ar}/^{39}\text{Ar}$  dating:

Chemical Geology, v. 145, p. 117–152.

Steiger, R. H. and Jaeger, E., 1977, Subcommission on Geochronology: convention on the use of decay constants in Geo and Cosmochronology: *Earth Planet. Sci. Lett.*, v. 36, p. 359–362.

Wijbrans, J. R., Pringle, M. S. Koppers, A. A. P. and Scheevers, R., 1995, Argon geochronology of small samples using the Vulkaan argon laserprobe: *Proc. Kon. Ned. Akad. Wet.*, v. 98, p. 185–218.

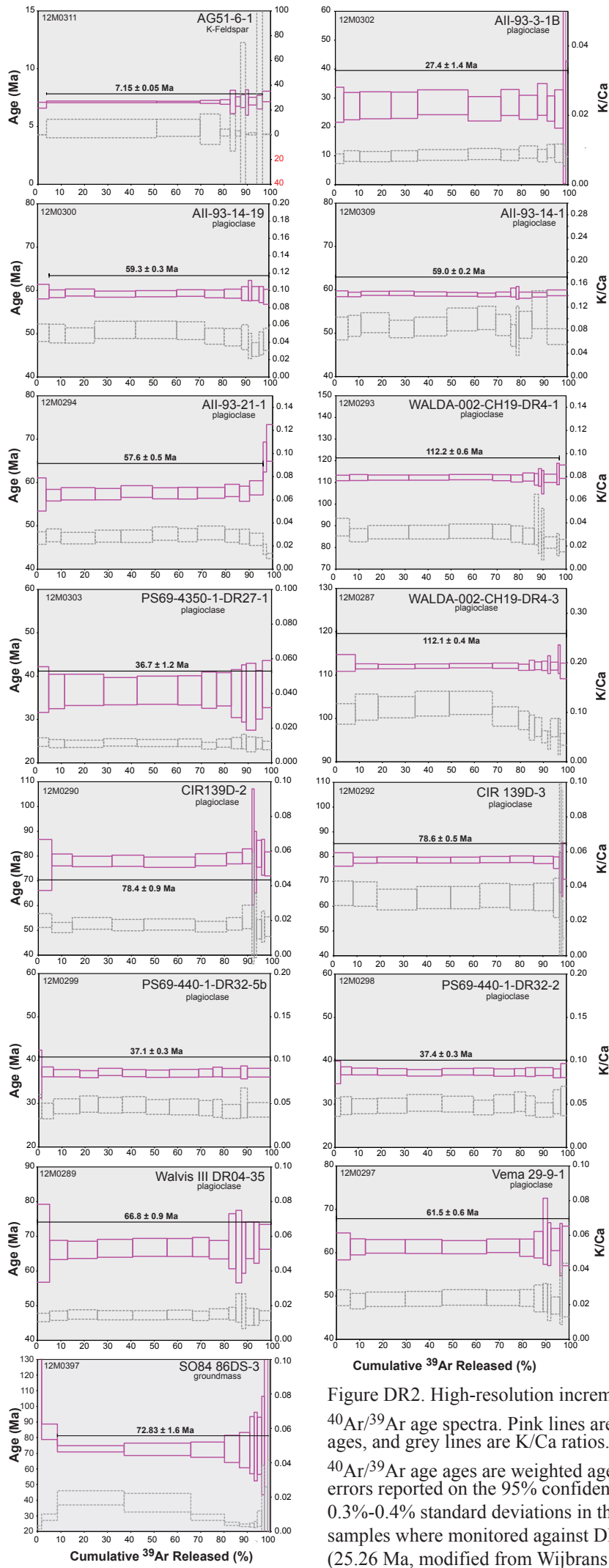


Figure DR2. High-resolution incremental heating  $^{40}\text{Ar}/^{39}\text{Ar}$  age spectra. Pink lines are  $^{40}\text{Ar}/^{39}\text{Ar}$  ages, and grey lines are K/Ca ratios. The reported  $^{40}\text{Ar}/^{39}\text{Ar}$  age ages are weighted age estimates with errors reported on the 95% confidence level, including 0.3%-0.4% standard deviations in the J- value. All samples were monitored against DRA monitor (25.26 Ma, modified from Wijbrans et al., 1995).